Cancer chemoprevention by the antioxidant Tempol

in cancer prone mice

Ralf Schubert[1,4], Laura Resor[1,4], Carrolee Barlow[2,6], Hiroyuki Yakushiji[1,5], Denise Larson[2], Angelo Russo[3], James B. Mitchell[3] and Anthony Wynshaw-Boris[1,2,7]

[1]Departments of Pediatrics, Medicine and the Comprehensive Cancer Center, UCSD School of Medicine

[2]Genetic Disease Research Branch, NHGRI, NIH

[3]Radiation Biology Branch, NCI

[4]These authors contributed equally.

Present addresses:

[5]Department of Surgery, Taku Hospital, Saga, Japan

[6]Salk Institute, La Jolla, CA

[7]To whom correspondence should be addressed at:
University of California, San Diego
School of Medicine
9500 Gilman Drive, Mailstop 0627
La Jolla, CA 92093-0627
Phone: (858) 822-3400
FAX: (858) 822-3409
email: awynshawboris@ucsd.edu

Reactive oxygen species (ROS) are important endogenous etiological agents for DNA damage [1], and recent studies have demonstrated a critical signaling function for ROS in mitogen-induced proliferation [2-6]. To test the effect of antioxidants as chemopreventative agents, we administered the nitroxide antioxidant Tempol (4-hydroxy-2,2,6,6-tetramethylpiperidine-N-oxyl) continuously in the diet of *Atm* and *p53* mutant mice, models of the human cancer prone syndromes ataxia-telangiectasia (AT) and Li-Fraumeni syndrome. Tempol treatment after weaning resulted in an increased lifespan of these mice by prolonging the latency to thymic lymphomas. Tempol treatment reduced ROS, tissue oxidative damage and stress, and induced a dose-dependent delay of G1 to S-phase progression. As expected for an agent affecting cell cycle progression, Tempol-treated mice are smaller, and do not display metabolic defects. Treatment of $Atm^{-/-}$ mice with another antioxidant, Vitamin E, reduced ROS, tissue oxidative damage, similar to Tempol. However, Vitamin E did not reduce oxidative stress, produce a cell cycle delay or increase the lifespan of these mice. These experiments provide strong evidence that nitroxide antioxidants can be used as novel chemopreventative agents in cancer prone syndromes, and we suggest that a likely mechanism of action is slowing of late G1 to S cell cycle progression.

Tempol was chosen for these experiments because: 1) it is one of a family of stable nitroxides that detoxify oxygen metabolites by redox cycling via one-electron

transfer reactions [7]; 2) it has SOD mimetic activity and confers catalase activity to heme proteins [8,9]; 3) it protects cells and animals from oxidative stress [10,11]; and 4) long-term treatment resulted in a reduction of tumor incidence in wild-type C3H mice [12]. We first tested *Atm*-deficient mice [13] since these mice: 1) display increased oxidative stress and damage [14-17]; 2) demonstrate a highly penetrant lymphoma phenotype [13]; 3) have a short latency tumors [13] ; and 4) are an excellent model of many aspects of the human disease ataxia-telangiectasia. Tempol was chronically administered in the diet of these animals to give a fairly constant dose throughout treatment. Because Tempol has a bitter, unpleasant taste to mice, it was mixed with bacon-flavored mouse chow at 58 mM (10 mg/g of food). $Atm^{-/-}$ mice were placed into one of three treatment arms: 1) mice fed bacon-flavored mouse chow without drug (control); 2) mice placed on Tempol-laced chow at weaning (Tempol at weaning); and mice born to females that were fed Tempol chow prior to mating, then constantly during pregnancy and lactation (Tempol at fertilization). Both treatment regimens resulted in an average serum concentration of 90-100 μM (data not shown). Combining both Tempol-treated groups, there was a significant increase in lifespan of Tempol-treated compared to control mice (40.7 vs. 30.1 weeks, $p<0.05$). When the Tempol groups were analysed separately, it was apparent that only mice treated at weaning had increased longevity. The mean survival time for animals treated with Tempol from fertilisation (Fig. 1a) was 37.1 weeks ($p>0.7$ vs. control), while the mean

survival time for animals treated with Tempol at weaning (Fig. 1b) was 62.4 weeks ($p<0.01$ vs. control).

To determine if Tempol plays a more general role in chemoprevention than simply reversing existing oxidative damage and stress in *Atm*-deficient mice, we also treated p53-deficient mice. Unlike *Atm* mice, *p53*-deficient mice have not been reported to display evidence of oxidative stress or damage [18,19], while both models exhibit DNA damage induced cell cycle checkpoint defects. Tempol was administered chronically only after weaning in four separate cohorts of $p53^{-/-}$ mice. Survival of Tempol-treated *p53*-deficient mice was found to be significantly increased ($p<0.05$) from 21.4 weeks to 25 weeks when all four studies were combined and analyzed (Fig. 1c). Thus, Tempol treatment resulted in significant chemoprevention in two mouse models of human cancer prone syndromes.

Most animals from each group were autopsied. As previously shown for *Atm*-deficient mice [13,20], all Tempol treated and control mice died from CD4+/CD8+ thymic lymphomas that contained 3-5 chromosomal translocations including both alleles of the TCR$\alpha\delta$ locus (data not shown). An early event in the development of thymic lymphomas in $Atm^{-/-}$ mice are chromosome 14 translocations that occur at the point of V(D)J recombination in the TCR$\alpha\delta$ locus [20]. These translocations occur during embryonic development well before Tempol treatment was initiated. Therefore, we determined

whether the early TCRαδ recombination event was affected by Tempol treatment *in vivo*. Splenocytes from untreated wild-type and *Atm*$^{-/-}$ mice or *Atm*$^{-/-}$ mice treated with Tempol for one month were examined for chromosome 14 translocations using green fluorescent labeled chromosome 14 painting probes (Fig. 2a-c). No translocations were observed in splenocytes induced to divide with the B cell mitogen lipopolysaccharide (data not shown). As expected, none of the untreated wild-type splenocytes, and 7.66% of untreated *Atm*$^{-/-}$ splenocytes induced to divide with the T-cell mitogen conconavalin A displayed chromosome 14 translocations (Fig. 2c). Importantly, conconavalin A induced splenocytes from *Atm*$^{-/-}$ mice fed Tempol did not display a decrease in the number of translocations on chromosome 14 (Fig. 2c). Finally, the lymphomas displayed by Tempol treated and control *p53* mutants displayed aneuploidy, as previously demonstrated for tumors from these mice [21]. These data are consistent with the interpretation that Tempol prolonged latency to tumors without affecting tumor type.

The chemopreventative effects of Tempol were associated with antioxidant effects. We directly determined the effect of Tempol treatment on intracellular ROS by measuring the conversion of non-fluorescent 2'7'-dichlorodihydrofluorescin to the fluorescent 2'7'-dichlorodihydrofluorescein (DCF) quantitatively by flow cytometry [22-24]. DCF fluorescence was significantly increased in thymocytes from *Atm*$^{-/-}$ mice relative to wild-type (Fig. 3a). Tempol significantly reduced DCF intensity in thymocytes from both wild-type and *Atm*$^{-/-}$ mice (Fig. 3a). Similar results were found with mitochondrial

membrane potential differences (data not shown), the first target of ROS-induced damage [25]. These data are consistent with the interpretation that there is an increase in ROS in cells from *Atm*$^{-/-}$ mice, and that Tempol treatment reduces ROS.

To test whether Tempol could not only reduce but also protect cells from ROS, wild-type and *Atm*$^{-/-}$ thymoctytes were treated with an extracellular oxidative insult, hypoxanthine and xanthine oxidase (HX/XO), in the presence or absence of Tempol, and cell viability was measured using an MTT (3-(4,5 dimethylthiazol-2-yl)-2,5-diphenyl tetrazolium bromide) viability assay [26]. After 18 hrs in culture, no toxic effects of Tempol were observed in wild-type and *Atm*$^{-/-}$ thymoctytes at concentrations up to 1 mM, although some toxicity was observed at 10 mM Tempol (data not shown). Tempol treatment (1 mM) resulted in significant protection to cells subjected to extracellular HX/XO oxidative stress after 4 hrs of treatment, with little toxic effect in the absence of oxidative stress (Fig. 3b). In addition, Tempol provided a slight but non-significant level of protection to thymocytes from *p53*$^{-/-}$ mice from oxidative insult by HX/XO (Fig. 2b), over a range of doses and concentrations (data not shown).

Markers of oxidative stress such as heme-oxygenase-1 (HO-1) are increased in brain tissue of *Atm*-deficient mice [14]. Consistent with this, Western blot analysis demonstrated increased levels of HO-1 protein in the thymus (the tissue where thymic lymphomas arise) of *Atm*-deficient mice compared with wild-type (Fig. 3c). Tempol treatment lowered these elevated levels of HO-1 in the thymus (Fig. 3c). To investigate

whether Tempol decreases oxidative damage, we performed Western blot analysis to detect carbonyl derivatives on oxidized proteins [27]. *Atm*-deficient thymus displayed markedly increased levels of oxidized proteins, while Tempol treatment lowered the levels of oxidative damage to proteins in the thymocytes of treated $Atm^{-/-}$ mice (Fig. 3d). As expected, *p53*-deficient mice did not display significant oxidative stress or damage compared to *Atm*-deficient control mice (Fig. 3c, d).

These data are consistent with the interpretation that the chemopreventative effects of Tempol reduced oxidative stress and damage, by reducing ROS, but they do not provide a mechanism for these effects. Since *Atm* and *p53* mutant mice display cell cycle checkpoint defects, we examined cell cycle populations after Tempol treatment. Cell cycle populations proved difficult to measure in thymocytes *in vivo* due to the low numbers of proliferating cells in the thymus. As a result, we used three actively proliferating *Atm*-deficient murine thymic lymphoma cell lines [20]. Surprisingly, we found a G1 to S cell cycle delay in these cells treated with Tempol. In unirradiated AT-4 cells, the fraction of cells in S-phase was reduced in a dose-dependent fashion by Tempol (Fig. 4a). There were significant differences in S phase fractions at Tempol concentrations above 1 mM, associated with an increase in cells in the G1 fraction, without change in the G2 fraction (Fig. 4a). Similar results were found in two other *Atm*-deficient thymoma cell lines AT-10 and AT-13 (data not shown), a lymphoma line derived from $p53^{-/-}$ mice (Fig. 4b), primary wild type splenocytes (Fig. 4c) and $Atm^{-/-}$ splenocytes (Fig. 4d).

Since Tempol caused a cell cycle delay, long-term treatment should chronically slow cellular proliferation, resulting in decreased overall size. A significant reduction in weight was observed in mice treated with Tempol at weaning (Fig. 5a) compared to mice fed Control food. An even greater reduction weight was seen in mice treated with Tempol from fertilization (Fig. 5a), compared to mice fed Tempol from weaning. There was also a trend in organ size reduction in the liver, kidney, spleen and thymus of treated mice, with no effect on overall cell size based on forward and side scatter analysis by flow cytometry (data not shown). To determine whether Tempol caused alterations in metabolism or activity, treated and control mice were further studied in CLAMS metabolic cages (Columbus Instruments). Wild-type mice were studied to eliminate confounding effects of genotype. Although Tempol treated mice drank more water (Fig. 5g), no differences were observed in O_2 consumption (Fig. 5b), CO_2 production (Fig. 5c), respiration rate (RER) (Fig. 5d), caloric heat output (Fig. 5e), food consumption (Fig. 5f), or activity (Fig. 5h-j) between Tempol treated and control mice. Similar results were found with *Atm*-deficient mice (data not shown).

To investigate whether other antioxidants displayed chemopreventative effects, $Atm^{-/-}$ mice were fed Vitamin E laced mouse chow after weaning. This treatment regimen has been shown previously to result in an average serum concentration of 39.6 μg/ml, which is approximately 10 mM [28]. In contrast to the effects of Tempol, we found that Vitamin E treatment did not increase the lifespan of these mice (Fig. 6a). This

anitoxidant has a similar antioxidant profile to Tempol, lowering intracellular ROS (Fig. 6b), protecting cells from an oxidative insult (Fig. 6c), and preventing oxidative damage *in vivo* (Fig. 6e). However, Vitamin E did not reduce oxidative stress *in vivo* (Fig. 6d) or produce a cell cycle delay *in vitro* even at concentrations far exceeding the expected serum concentration range we expected to achieve *in vivo* (Fig. 6f). As expected for a compound that does not produce a cell cycle delay, the weight of Vitamin E treated mice did not differ from control mice (Fig. 6g).

Long-term administration of the nitroxide Tempol via the diet after weaning increased the latency to thymic lymphomas in two mouse models of human tumor prone syndromes, *Atm* and *p53*-deficient mice, without a change in the tumor type characteristic of these tumor prone models. Tempol treatment reduced ROS, tissue oxidative damage and oxidative stress in *Atm* mutant mice *in vivo* and protected thymocytes from gamma-irradiation induced DNA double strand breaks and oxidative stress *in vitro*. Vitamin E had a some effects similar to Tempol but did not produced a cell cycle delay or increase the lifespan of the $Atm^{-/-}$ mice, suggesting that the most likely mechanism of action for chemoprevention by Tempol is due to a delay in cell cycle progression. The novel effect of Tempol on cell cycle progression also occurred within the concentration range we were able to achieve *in vivo*.

Although weight reduction and caloric restriction has been shown to increase latency to cancer in tumor-prone mice [29], this effect cannot completely explain the

effectiveness of Tempol in these experiments. Mice treated with Tempol from fertilization were much smaller than the other two groups of mice, yet there was no effect on latency to tumors in this group. The latter group displayed more severe side effects in general, such as embryonic and perinatal lethality and hyperactivity, consistent with a cell cycle effect during development. These adverse effects were not noted in mice treated with Tempol at weaning, nor were they noted in a large cohort of C3H mice treated after weaning throughout their lifetime with similar Tempol doses [12]. Further, the food consumption and metabolic rate for mice treated with and without Tempol was similar (Fig. 5e,f). It should be noted that previous studies [30,31] suggested that high concentrations of Tempol could decrease the number of tumor cells in S and G2/M phase due to apoptosis. However, we did not observe apoptotic or necrotic cell death at any doses tested.

Overall, these studies point to a novel use of nitroxides such as Tempol in the chemoprevention of cancer in *Atm* and *p53*-deficient mice. In the absence of ATM and p53, normal cell cycle control has been lost. Treatment of these mice with Tempol results in a delay in progression from G1 to S phase of the cell cycle, causing a slowing of cellular proliferation and prolonged latency to tumor formation. This may act either to artificially restore a defective cell cycle checkpoint or generally prolong the cell cycle. The apparent greater effect on survival in *Atm*-deficient mice may also result from the additional effect of Tempol to decrease oxidative stress and damage found in these mice.

Since the *Atm*- and *p53*- deficient mice are good models of many aspects of human AT and Li-Fraumeni syndrome, our results raise the possibility that Tempol could be used in the chemoprevention of tumors in humans with cancer prone syndromes, and may be especially effective in ones that result from oxidative stress and cell cycle checkpoint-deficient mechanisms.

METHODS

Mice and Tempol treatment

Atm-deficient mice [13] and *p53*-deficient mice (Jackson Labs), in 129SvEv background, were used and all animal procedures were performed according to protocols approved by both the NIH ACUC and the UCSD Animal Subjects Committee. Powdered Tempol was mixed with bacon-flavored mouse chow (Bio-Serv, NJ) at a concentration equivalent to 58 mM (10 mg/g of food). Sixty seven $Atm^{-/-}$ mice (32 males and 35 females) were separated into three groups: 40 mice (22 males and 18 females) received bacon-flavored control chow; 17 mice (5 males and 12 females) were treated with Tempol started in the females prior to mating; 10 mice (5 males and 5 females) were treated with Tempol starting at weaning (3 weeks old). Sixty-nine $p53^{-/-}$ mice were fed either Tempol or control food in four different cohorts. Overall, 38 mice were fed Tempol-treated and 31 were fed control food (7 Tempol-treated and 6 control mice in the first, 11 Tempol-treated and 10 control-fed mice in the second, 10 Tempol-treated and 10 control-fed mice in the third, and 10 Tempol-treated and 5 control-fed mice in the fourth cohort).

Vitamin E treatment of *Atm*$^{-/-}$ mice

Vitamin E food was prepared according to Tsimikas et al.[28]. *Atm*-deficient mice [13] were treated after weaning (10 Vitamin E and 10 Control). The protocol for Tempol treatment, as described above, was followed to monitor Vitamin E treated mice.

Analysis of chromosome 14 translocations

Splenocytes from mice treated with Tempol at weaning for one month or from untreated age-matched *Atm*$^{-/-}$ or wild-type mice were isolated and cultured in RPMI 1640 supplemented with 10% FCS, 1% penicillin/streptomycin, 1% HEPES, 2% glutamine, 0.2% gentamycin and 50 U/ml IL-2 for 48 hrs in the presence of 6 μg/ml con A or 25 μg/ml LPS. After 60 min incubation in 10 μg/ml demecolcine, cells were harvested in 0.075 M KCl for 30 min and fixed in 3:1 methanol:acetic acid. Metaphase spreads were prepared and chromosomes were stained with mouse chromosome 14-specific paint probes (Cambio) according to the manufacturer's protocol. Spreads were counterstained with DAPI and mounted with Vectashield antifade medium (Vectashield).

Measuring intracellular ROS in thymocytes

Thymi were isolated from one-month-old *Atm*$^{+/+}$ and *Atm*$^{-/-}$ mice. Cells were untreated, treated with 10 μM Tempol or Vitamin E for 30 min, collected and

resuspended in 1 ml PBS containing 10 μM 2'7'-dichlorodihydrofluorescin diacetate (Molecular Probes, Inc., OR) for 30 min. Cells were labelled with PE-αCD4 and APC-αCD8a (BD PharMingen, CA), stained with 7AAD, and analyzed by flow cytometry on a Coulter Epics Elite (Beckman Coulter, Inc., CA). The FITC signals from DCF in live cells were determined for CD4/CD8 double positive cells, since this is the population from which tumors arise [13,20]. Six independent experiments were performed.

Cell culture

Isolated thymocytes were cultured as stated above. Hypoxanthine/xanthine oxidase (HX/XO) was used for induction of oxidative stress. To verify that H_2O_2 as well as $\bullet O^{2-}$ was produced by HX/XO, catalase (Boehringer Mannheim, Germany) and SOD (Roche Molecular Biochemicals, IN) were used as controls in each experiment.

MTT assay

Thymocytes were treated with 0.1 mM HX (Sigma, St. Louis, MO), 10 mU XO (Boehringer Mannheim, Germany) with and without 1 mM Tempol or Vitamin E for 4 and 18 hrs. PBS with 0.5 mg/ml MTT (Sigma, MO) was added and the cells were incubated further for 4 hrs at 37°C [26].

Western Blot Analysis

Thymi of age-matched mice, fed Tempol, Vitamin E or control food, were used for analysis of HO-1 protein expression by Western blot analysis according as previously described [32]. Protein was electrophoresed on a 4% to 20% Tris-glycine gel (Invitrogen, CA), and transferred to polyvinylidene difuoride membranes (Millipore, MA). Primary antibodies HO-1 (Stressgen SPA-895) and Actin (Santa Cruz Biotech: Santa Cruz, CA, sc-1616) were incubated at 1:500 in 3% milk TBS-T overnight at 4°C. Following incubation with peroxidase-conjugated secondary antibodies (1:5000) the proteins were visualized by chemiluminescence detection system (Pierce Super Signal West Pico: Pierce, IL).

To detect the level of oxidized proteins, we used the Intergen Oxyblot kit (according to the manufacturer's protocol) to assess the level of oxidized protein carbonyl groups. Protein samples were prepared from age matched mice fed control or Tempol-treated food as stated above. A non-derivatized negative control was run to ensure that non-specific bands were not being detected.

Cell cycle analysis

Splenocytes were isolated from age-matched wild type and *Atm*-deficient mice and cultured as stated above. Unirradiated $Atm^{-/-}$ thymoma cells (AT-4, AT-10 and AT-13) were treated with different Tempol or Vitamin E concentrations (0, 0.01, 0.1, 1.0, 10

mM) for 1.5 hrs in the presence of 10 μM BrdU, harvested, fixed for 45 min and treated with 2N HCl for 30 min. Cells were stained with FITC-conjugated mouse anti-BrdU antibody (BD PharMingen), cells were analyzed by flow cytometry. Cell cycle distribution was performed using Coulter Epics Elite software version 4.1 (Coulter, Inc.). Propidium iodide analysis and trypan blue staining were performed to analyse apoptotic and necrotic cells, respectively.

Metabolic Measurements

Six pairs of age matched wild-type mice from the Tempol and Control food groups were placed in CLAMS metabolic cages (Columbus Instruments). These metabolic chambers monitor activity, food and water consumption, and metabolic performance. Data was collected every 30 minutes over three 12-hour dark cycles and two 12-hour light cycles. The metabolic measurements included the volume of carbon dioxide produced (VCO2) the volume of oxygen consumed (VO2), the respiration measurement (RER=VCO2/VO2), and the caloric (heat) value ((3.815 + 1.232 x RER) x VO2). The data is represented as the mean values over each twelve-hour period.

Statistical analysis

Survival time of mice was used to generate Kaplan-Meier survival curves that were compared using log-rank (Mantel-Cox) test. A Cox proportional-hazard regression

analysis was used to adjust for the potential effect of gender. A two factorial analysis of variance (ANOVA) (genotype × treatment) were used to analyse data from immunohistochemistry and measuring intracellular ROS in thymocytes. Post-hoc comparisons were made using Scheffe's F and Fisher's protected least significant difference (PLSD) test for measuring intracellular ROS in thymocytes, respectively. For the MTT assay and cell cycle analysis an unpaired Student's T-test was performed.

Acknowledgements

We would like to thank Judy Nordberg at the San Diego VA Hospital FACS Core for help and advice with flow cytometry, Jeff Long for assistance with the CLAMS experiments, Amy Sullivan, Jennifer MacArthur, and Scott Barlow for technical help, and Web Cavenee, Geoff Rosenfeld and Yutaka Sagara for advice and comments on the manuscript. This work was supported by intramural funds from the NHGRI, institutional funds from UCSD School of Medicine, and an institutional grant from HHMI.

Competing interests statement: The authors declare that they have no competing financial interests.

Correspondence and requests for material should be addressed to A.W.B. (awynshawboris@ucsd.edu).

REFERENCES

1. Beckman, K.B. & Ames, B.N. Oxidative decay of DNA. *J Biol Chem* **272**, 19633-6. (1997).
2. Burdon, R.H. Superoxide and hydrogen peroxide in relation to mammalian cell proliferation. *Free Radic Biol Med* **18**, 775-94. (1995).
3. Schmidt-Ullrich, R.K., Dent, P., Grant, S., Mikkelsen, R.B. & Valerie, K. Signal transduction and cellular radiation responses. *Radiat Res* **153**, 245-57. (2000).
4. Pearce, A.K. & Humphrey, T.C. Integrating stress-response and cell-cycle checkpoint pathways. *Trends Cell Biol* **11**, 426-33. (2001).
5. Finkel, T. Reactive oxygen species and signal transduction. *IUBMB Life* **52**, 3-6. (2001).
6. Leroy, C., Mann, C. & Marsolier, M.C. Silent repair accounts for cell cycle specificity in the signaling of oxidative DNA lesions. *EMBO J* **20**, 2896-906. (2001).
7. Krishna, M.C., Grahame, D.A., Samuni, A., Mitchell, J.B. & Russo, A. Oxoammonium cation intermediate in the nitroxide-catalyzed dismutation of superoxide. *Proc Natl Acad Sci U S A* **89**, 5537-41. (1992).
8. Samuni, A., Krishna, C.M., Riesz, P., Finkelstein, E. & Russo, A. A novel metal-free low molecular weight superoxide dismutase mimic. *J Biol Chem* **263**, 17921-4. (1988).
9. Krishna, M.C. et al. Stimulation by nitroxides of catalase-like activity of hemeproteins. Kinetics and mechanism. *J Biol Chem* **271**, 26018-25. (1996).
10. Mitchell, J.B. et al. Biologically active metal-independent superoxide dismutase mimics. *Biochemistry* **29**, 2802-7. (1990).
11. Rak, R. et al. Neuroprotection by the stable nitroxide Tempol during reperfusion in a rat model of transient focal ischemia. *J Neurosurg* **92**, 646-51. (2000).
12. Mitchell, J.B. et al. A low molecular weight antioxidant decreases weight and lowers tumor incidence. *Free Radic Biol Med* **34**, 93-102. (2003).
13. Barlow, C. et al. Atm-deficient mice: a paradigm of ataxia telangiectasia. *Cell* **86**, 159-71. (1996).
14. Barlow, C. et al. Loss of the ataxia-telangiectasia gene product causes oxidative damage in target organs. *Proc Natl Acad Sci U S A* **96**, 9915-9. (1999).

15. Kamsler, A. et al. Increased oxidative stress in ataxia telangiectasia evidenced by alterations in redox state of brains from Atm-deficient mice. *Cancer Res* **61**, 1849-54. (2001).
16. Quick, K.L. & Dugan, L.L. Superoxide stress identifies neurons at risk in a model of ataxia- telangiectasia. *Ann Neurol* **49**, 627-35. (2001).
17. Stern, N. et al. Accumulation of DNA damage and reduced levels of nicotine adenine dinucleotide in the brains of Atm-deficient mice. *J Biol Chem* **277**, 602-8. (2002).
18. Abraham, R.T. Cell cycle checkpoint signaling through the ATM and ATR kinases. *Genes Dev* **15**, 2177-96. (2001).
19. Kastan, M.B. & Lim, D.S. The many substrates and functions of ATM. *Nat Rev Mol Cell Biol* **1**, 179-86. (2000).
20. Liyanage, M. et al. Abnormal rearrangement within the alpha/delta T-cell receptor locus in lymphomas from Atm-deficient mice. *Blood* **96**, 1940-6. (2000).
21. Purdie, C.A. et al. Tumour incidence, spectrum and ploidy in mice with a large deletion in the p53 gene. *Oncogene* **9**, 603-9. (1994).
22. Burow, S. & Valet, G. Flow-cytometric characterization of stimulation, free radical formation, peroxidase activity and phagocytosis of human granulocytes with 2,7-dichlorofluorescein (DCF). *Eur J Cell Biol* **43**, 128-33. (1987).
23. Watanabe, S. In vivo fluorometric measurement of cerebral oxidative stress using 2'- 7'-dichlorofluorescein (DCF). *Keio J Med* **47**, 92-8. (1998).
24. Wang, H. & Joseph, J.A. Quantifying cellular oxidative stress by dichlorofluorescein assay using microplate reader. *Free Radic Biol Med* **27**, 612-6. (1999).
25. Melov, S. Therapeutics against mitochondrial oxidative stress in animal models of aging. *Ann N Y Acad Sci* **959**, 330-340. (2002).
26. Mossmann. Rapid colorimetric assay for cellular growth and survival: application to proliferation and cytotoxicity assays. *Journal of Immunological Methods* **65**, 55-63 (1983).
27. Singhal, A.B., Dijkhuizen, R.M., Rosen, B.R. & Lo, E.H. Normobaric hyperoxia reduces MRI diffusion abnormalities and infarct size in experimental stroke. *Neurology* **58**, 945-52. (2002).
28. Tsimikas S, S.B., Witztum JL, Palinski W. In vivo uptake of radiolabeled MDA2, an oxidation-specific monoclonal antibody, provides an accurate measure of atherosclerotic lesions rich in oxidized LDL and is highly sensitive to their regression. *Arterioscler Thromb Vasc Biol.* **20**, 689-97 (2000).
29. Pugh, T.D., Oberley, T.D. & Weindruch, R. Dietary intervention at middle age: caloric restriction but not dehydroepiandrosterone sulfate increases lifespan and lifetime cancer incidence in mice. *Cancer Res* **59**, 1642-8. (1999).

30. Gariboldi, M.B. et al. Antiproliferative effect of the piperidine nitroxide TEMPOL on neoplastic and nonneoplastic mammalian cell lines. *Free Radic Biol Med* **24**, 913-23. (1998).
31. Monti, E. et al. Nitroxide TEMPOL impairs mitochondrial function and induces apoptosis in HL60 cells. *J Cell Biochem* **82**, 271-6 (2001).
32. Sambrook, J., Fritsch, E.F. & Maniatis, T. *Molecular cloning: A Laboratory Manual*, (Cold Spring Harbor Laboratory Press, 1989).

Figure Legends

Figure 1

Kaplan-Meier analysis for tumor-free survival of *Atm*$^{-/-}$ mice (**a, b**) or *p53*$^{-/-}$ mice (**c**) fed food with (dashed line) and without (solid line) Tempol from before fertilization (**a**) or after weaning (**b, c**).

Figure 2

Aberrations of chromosome 14 were detected in *Atm*$^{-/-}$ mouse splenocytes by a specific chromosome 14 paint probe (green) (**a-c**). Chromosomes were counterstained with DAPI (blue). Representative metaphase nuclei without (**a**) and with (**b**) a chromosome 14 translocation are shown. (**c**), Number of chromosome 14 translocations in untreated and Tempol treated *Atm*$^{-/-}$ mice and untreated *Atm*$^{+/+}$ animals. Splenocytes were cultured with conconavalin A to stimulate T cell proliferation. Data represent three independent experiments for each group and treatment. (* $p < 0.05$; ** $p < 0.01$).

Figure 3

(**a**), Levels of reactive oxygen species (ROS) measured by mean DCF fluorescence in primary thymocytes from wild-type, *Atm*$^{-/-}$ and *p53*$^{-/-}$ mice treated with (gray) and without (black) Tempol, and represented as fold change from wild-type control samples. (**b**),

MTT survival analysis of primary thymocytes from wild-type (white), *Atm*$^{-/-}$ (black) and *p53*$^{-/-}$ (gray) mice that were untreated (Medium), treated with Tempol (Tempol), treated with an extracellular oxidative insult (HX/XO), and treated with an oxidative insult plus Tempol (HX/XO + Tempol). Levels of oxidative stress (**c**) and oxidative damage (**d**) in the thymus of control and Tempol treated mice were measured by Western blot analysis of HO-1 levels (**c**) and protein carbonyl groups (**d**).

Figure 4

Cell cycle analysis in the *Atm*-deficient lymphoma cell line AT4 (**a**), a *p53*-deficient lymphoma cell line (**b**), wild-type (**c**) and *Atm*-deficient splenocytes (**d**) stimulated with concanavalin A. Graphs display the mean ± SEM change of cell numbers in G1-, S-, and G2-phase after treatment with increasing concentrations of Tempol. Percentage of S-phase cells in primary splenocytes is presented by the second y-axis to the right side of the plot. Data represent three independent experiments for each group and treatment. (* p <0.05).

Figure 5

(**a**), Significant weight reduction in Tempol treated at weaning (black squares), Tempol treated at fertilization (black diamonds) compared to control (open circles) *Atm*$^{-/-}$ mice. Significance between weights is denoted by (**1**) comparing to *Atm*$^{-/-}$ mice fed control food

and (2) comparing to *Atm*$^{-/-}$ mice treated at weaning. (**b-j**), Metabolic parameters were measured over three days using CLAMS metabolic cages (Columbus Instruments) for wild-type mice treated with (open circles, n=4) and without Tempol (closed circles, n=3). X-axis displays two light cycles (L1-L2) and three dark cycles (D1-D3). (**b**), Total oxygen consumed; (**c**), CO2 production; (**d**), respiration index (RER); (**e**), caloric (heat) production; (**f**), food consumption; (**g**), water consumption; (**h**), long axis movement; (**i**), short axis movement; and (**j**), vertical axis movement (rearing).(* p <0.05; ** p <0.01; *** p <0.005).

Figure 6

(**a**), Kaplan-Meier analysis of tumor free survival for *Atm*$^{-/-}$ mice fed food with (solid line) and without (dashed line) Vitamin E after weaning. (**b**), Levels of reactive oxygen species (ROS) measured by mean DCF fluorescence in primary thymocytes from wild-type and *Atm*$^{-/-}$ mice treated without (black), with 0.01 mM (gray), and 0.1 mM (clear) Vitamin E, and represented as fold change from wild-type control samples. (**c**), MTT survival analysis of primary thymocytes from wild-type (white) and *Atm*$^{-/-}$ (grey) mice that were untreated (Medium), treated with an extracellular oxidative insult (HX/XO), treated with an oxidative insult plus Vitamin E (HX/XO + Vit. E) and treated with oxidative insult plus Tempol (HX/XO + Tempol). Levels of oxidative stress (**d**) and oxidative damage (**e**) in the thymus of control and Tempol treated mice were measured by Western blot analysis of HO-1 levels (**e**) and protein carbonyl groups (**e**). (**f**) Cell

cycle analysis in the *Atm*-deficient lymphoma cell line AT4 treated with increasing concentrations of Vitamin E. Graphs display the mean ± SEM change of cell numbers in G1-, S-, and G2-phase after treatment. Data represent three independent experiments for each group and treatment. (g) Weight of $Atm^{-/-}$ mice fed Vitamin E (black squares) or control food (open circles). (* $p < 0.05$).

Figure 1- *Schubert et al.*

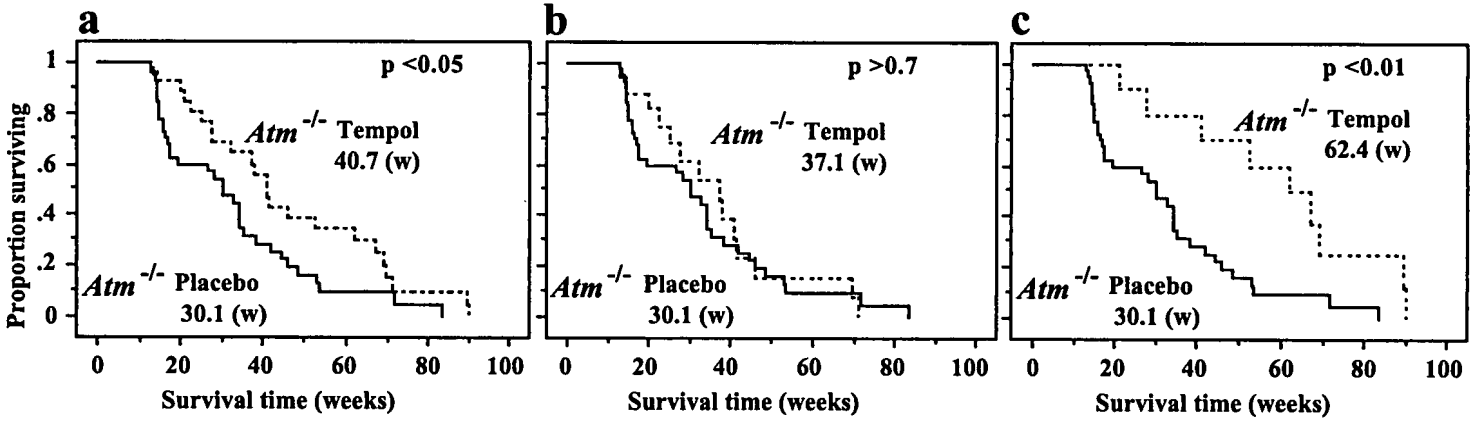

Figure 2- *Schubert et al.*

a

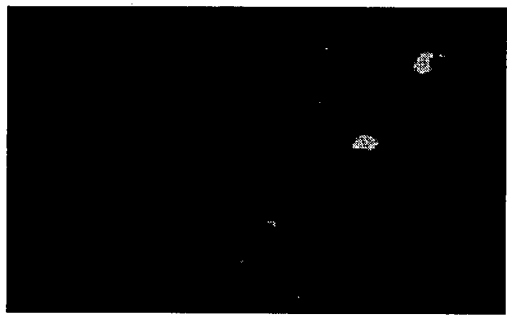

b

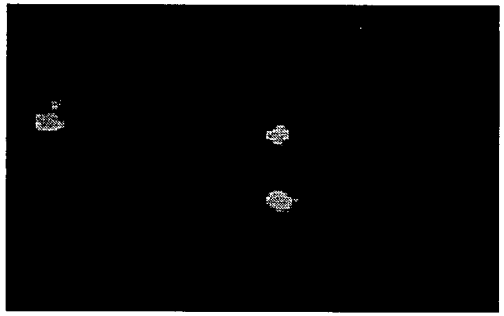

c

	Treatment	MPS counted	Translocations	Percentage	SEM
$Atm^{+/+}$	Control	86	0	0	0
$Atm^{-/-}$	Control	502	36	7.66	0.30
$Atm^{-/-}$	Tempol	355	25	7.58	0.88

Figure 3 - *Schubert et al.*

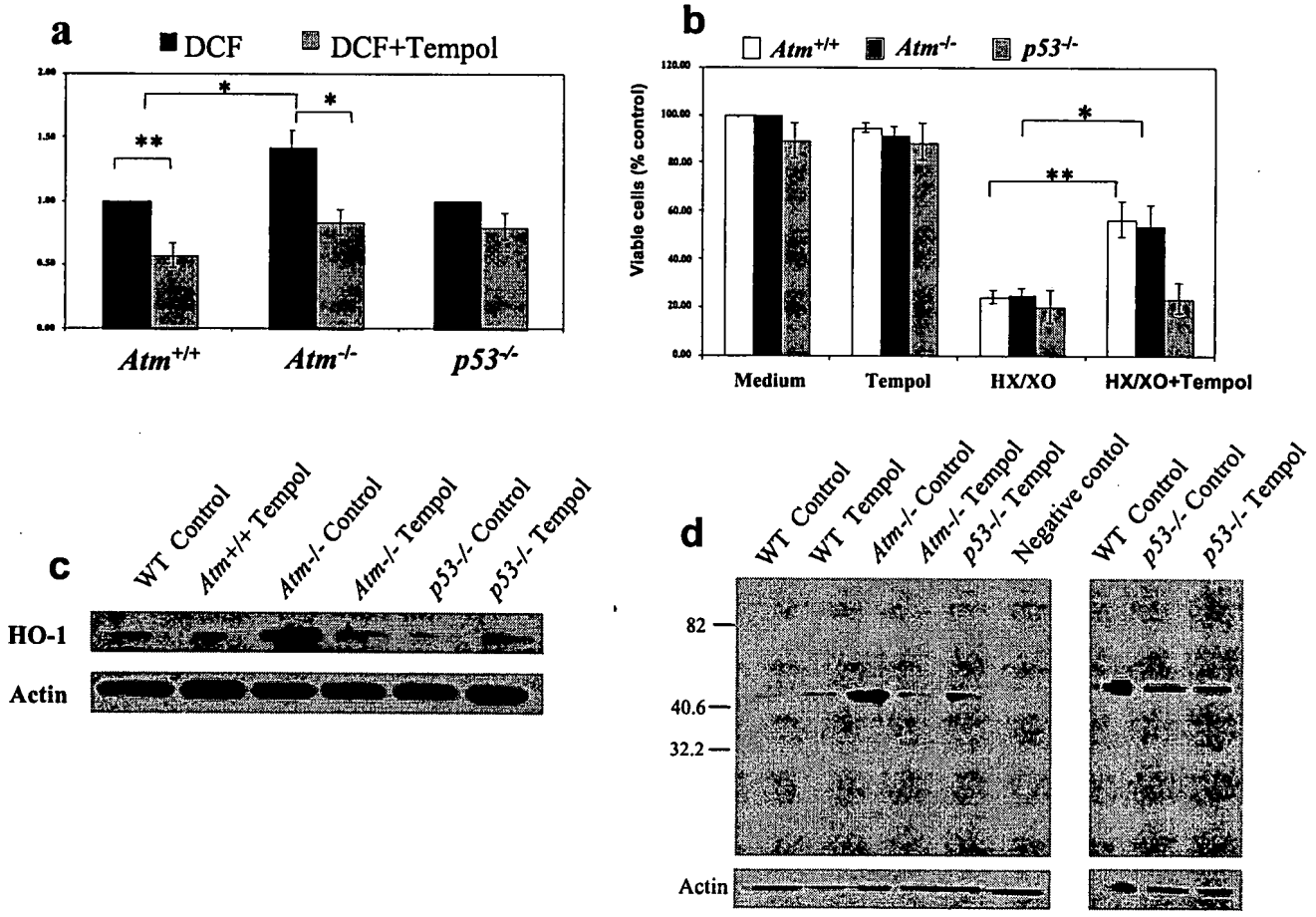

Figure 4 - *Schubert et al.*

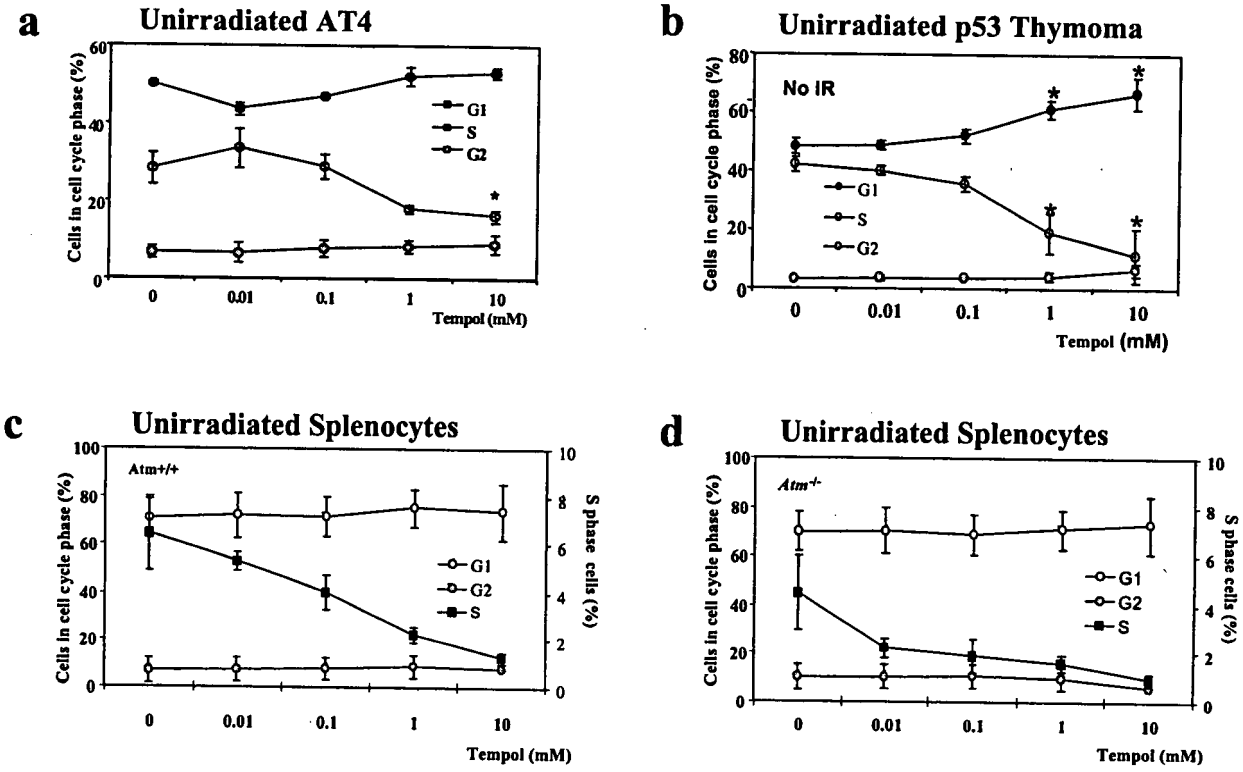

Figure 5- *Schubert et al.*

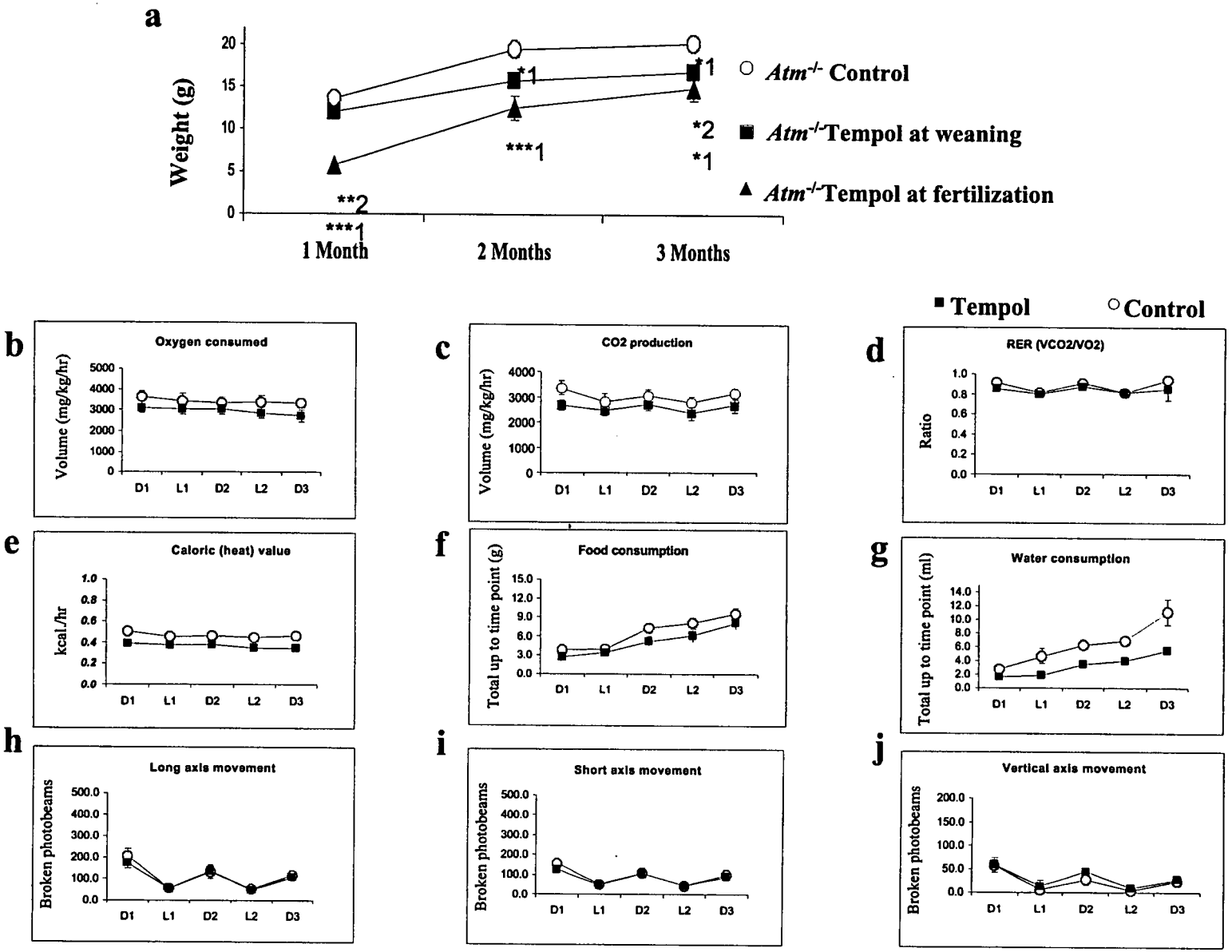

Figure 6 -*Schubert et al.*